Research Square

Preprints are preliminary reports that have not undergone peer review.
They should not be considered conclusive, used to inform clinical practice,
or referenced by the media as validated information.

High Performance O-Band PDFA Design and Performance Analysis for Next-Generation Data Center Connections

Hasan CIHANGIR

cihangir@harran.edu.tr

Harran University

Murat YUCEL

Gazi University

Bengisu UNALAN

TED University

Ozcan AKCESME

Gazi University

Pouria PISHGAM

Gazi University

Ayten DINCER

Hugo Brennenstuhl GmbH & Co

Vehbi YOLCU

Kütahya Dumlupınar University

Zuhal ASLAN AKYOL

Kastamonu University

Research Article

Keywords: Double-pass configuration, Bi-directional configuration, PDFA, optical gain, noise figure, optimization

Posted Date: May 20th, 2026

DOI: https://doi.org/10.21203/rs.3.rs-9615674/v1

License: This work is licensed under a Creative Commons Attribution 4.0 International License.
Read Full License

Additional Declarations: No competing interests reported.

High Performance O-Band PDFA Design and Performance Analysis for Next-Generation Data Center Connections

Corresponding author: Hasan CIHANGIR

Hasan CIHANGIR [a], Murat YUCEL [b,c] , Bengisu UNALAN [d] Ozcan AKCESME [b], Pouria PISHGAM [b,c], Ayten DINCER [e], Vehbi YOLCU [f], Zuhal ASLAN AKYOL [g]

cihangir@harran.edu.tr

muyucel@gazi.edu.tr

bengisu.unalan@tedu.edu.tr

ozcanakcesme@gazi.edu.tr

pouria.pishgam1@gazi.edu.tr

ayten.dincer@brennenstuhl.de

vehbi.yolcu@dpu.edu.tr

zuhalaslan@kastamonu.edu.tr

[a] Harran University, Department of Electrical-Electronics Engineering, Şanlıurfa, Türkiye

[b] Gazi University, Graduate School of Natural and Applied Sciences, Department of Electrical-Electronics Engineering, Ankara, Türkiye

[c] Gazi University, Faculty of Technology, Department of Electrical-Electronics Engineering, Ankara, Türkiye

[d] TED University, Department of Electrical and Electronics Engineering, Ankara, Turkey

[e] Hugo Brennenstuhl GmbH & Co, Tübingen, Germany

[f] Kütahya Dumlupınar University, Simav Faculty of Technology, Department of Software Engineering, Kütahya, Türkiye

[g] Kastamonu University, Department of Computer Technologies, Kastamonu, Türkiye

Abstract

For O-band applications requiring high-speed transmission, such as data center interconnections (DCI), 5G infrastructures, and AI clusters, developing new configurations of praseodymium doped fiber amplifier (PDFA) and determining their main parameter values is crucial with respect to both gain and cost. Furthermore, the main parameters, namely praseodymium doped fiber (PDF) length, input signal power, and pump laser power, are very important for PDFA designs. This study presents the simulation, optimization, and analysis of the traditional bidirectional PDFA (BD-PDFA) configuration and, for the first time in the literature, the double-pass PDFA (DP-PDFA) (one-stage) configuration proposed as an alternative. Here, these parameters, specifically gain and noise factor (NF), are analyzed comparatively for two amplifiers. Additionally, for the second window, the O-band, gain and NF are examined for the 1270–1340 nm band range. Subsequently, the power conversion effect (PCE) and amplified spontaneous emission (ASE) noise power are compared. As a result of the optimized parameter values, the optimum gain obtained for BD-PDFA is 41,39 dB, and the NF at this point is around 5,53 dB. For DP-PDFA, the maximum gain is 47,42 dB, and the NF at this point is around 5,65 dB. Overall, when looking at the both amplifier configurations, with respect to gain for the 1310 nm signal wavelength, DP-PDFA performed significantly better than BD-PDFA by approximately 6 dB. Furthermore, with respect to NF at this point, the values for the two amplifiers were found to be very similar. From a design perspective, the proposed DP-PDFA system was found to be much more efficient. In conclusion, it was found that using the newly proposed DP-PDFA configuration system instead of the BD-PDFA system is more appropriate.

Keywords: Double-pass configuration, Bi-directional configuration, PDFA, optical gain, noise figure, optimization

1. Introduction

In recent years, the demand for internet traffic has increased exponentially due to the increase in the number of users on both wired and wireless platforms. This increase stems from applications requiring high bandwidth, such as the widespread adoption of 5G technology, the development of online services, social networking platforms, high-definition video streaming, cloud-based gaming services, and e-commerce platforms (Kanwal et al. 2022; Winzer et al. 2018; Ferrari et al. 2020; Mirza et al. 2020; Chen et al. 2016).

Today, optical communication networks play a critical role in meeting these increasing traffic demands and ensuring the sustainability of global data transmission (Krishna et al. 2025; Elson et al. 2024). Two major wavelength ranges are used for fiber optical communications using fiber optics, namely, the C-band, which refers to a wavelength of 1550 nm and the O-band, which refers to a wavelength of 1310 nm. These two bands have minimum attenuation due to scattering and absorption losses, at ~0.22 dB/km versus ~0.3 dB/km respectively (Ferrari et al. 2020; Hui 2019). Although the lowest transmission loss occurs in the C-band, the efficient use of new optical windows has become essential as this region approaches its capacity limits (Rapp and Eiselt 2021).

In this context, interest in the 1300 nm window is increasing due to its low attenuation of 0.3 dB/km and the zero dispersion point of single-mode fibers (SMF) in the ITU-T G.652 standard being in this region (Luo et al. 2012). This low chromatic dispersion characteristic of the O-band (1260-1360 nm) enables high-speed transmission by minimizing distance-dependent signal distortions. It offers cost-effective solutions by reducing system complexity and high-power consumption. The O-band constitutes an ideal environment for short-range lines up to 40 km connecting radio units and baseband units in DCI, Passive Optical Networks (PON/FTTx) and 5G networks. In addition, it finds application in high-speed Ethernet standards such as 100GBASE-LR4 and 400GBASE-LR8 by supporting low-latency connections between Artificial Intelligence (AI) clusters and GPUs in edge computing. PDFA is considered the primary amplification choice for optical transmission systems operating in the O-band (Mirza et al. 2021). Offering a commercially accessible solution in the O-band, PDFA is critical in overcoming the capacity challenges of future optical networks. Consequently, research into new configurations of PDFAs is crucial for establishing scalable and high-performance infrastructures in the face of increasing data volumes.

The primary purpose of commercial PDFAs is to operate at the O-band's 1300 nm optical range and be instrumental in addressing the future network's bandwidth and capacity deficiencies (ThorLabs.; Fiberlabs Inc.; Alharbi et al. 2022). PDFAs will also be utilized in other advanced applications, such as high-power fiber lasers, non-linear optical frequency conversion, materials processing, and the coherent formation of signal beams, in addition to providing O-band data communication, 400G/800G transceiver testing, overload testing of O-band receivers, and coarse wavelength division multiplexing (CWDM) testing and silicon photonic device characterization. (ThorLabs.; Cumberland et al. 2007; Webber 2012; He et al. 2006). In addition to their use in next-gen data centers with low-power O-band coherent links, PDFAs also have applications in Ethernet (GbE, 10 GbE and 100 GbE) fiber to the home (FTTH), video transmission, CATV networks, SONET/SDH systems and network monitoring processes (Fiberlabs Inc.; Maharry et al. 2023). These broad technical capabilities offered by PDFAs allow the devices to be used in a wide range of fields, from academic research to highly automated industrial production lines (Fiberlabs Inc.).

However, the low gain and efficiency of traditional amplifiers make large-scale system integration difficult. Therefore, current research focuses on new PDFA configurations that offer high performance to increase amplifier efficiency.

Generally, bidirectional pumping is preferred among forward, backward, and bidirectional pumping to increase amplifier gain. A review of the literature reveals a focus on bidirectional and double-pass (two-stage) pumping configurations.

Alharbi et al. presented a simulation study based on a bidirectional pumping scheme to improve the small signal gain, PCE, and output optical power performance of PDFAs operating in the O-band (1270–1350 nm) (Alharbi et al. 2022). Obaid et al. demonstrated two different thulium-doped fiber amplifier (TDFA) configurations (two-stage-double-pass and bidirectional TDFA arrangements), each optimized with a multi-parameter optimization algorithm (Obaid et al. 2024). Wu et al. primarily investigated the amplification effect of TDFA at a wavelength of 2 μm. They compared the different amplification effects of single-stage, two-stage, and three-stage TDFAs

under appropriate conditions (Wu et al. 2025). Ali et al. experimentally validated broadband amplification using a series hybrid fiber amplifier. They improved the flatness gain bandwidth using the double-pass method for erbium and Raman amplifiers (Ali et al. 2022). Gürkaynak et al. showed experimentally that a double-pass hybrid prism fiber amplifier can obtain wide amplification flatness bandwidth. The suggested design consists of two different types of fibers (series erbium-Raman amplifier on one side and Raman amplifier on the other side) (Gurkaynak et al. 2021). Ali et al. simulated and experimentally validated the effect of gain control techniques on gain level and pump power optimization in a double-pass parallel hybrid fiber amplifier using Optisystem (Ali et al. 2020). Khan et al. compared forward, backward, and bidirectional TDFA configurations focusing on the parametric and schematic optimization of TDFAs. They reported that optimum gain was obtained with bidirectional TDFA (Khan and Gurjar 2022). Mirza et al. published an article describing an increased performance of a YDFA operating in the 1.02 - 1.08 μm spectral range utilizing an optimized two-stage double-pass pumping configuration that was designed specifically for use with asymmetrical bands (Mirza et al. 2022).Wang et al. evaluated and improved the gain and noise properties of Bi-DFA in the O-Band with three separate pump types (forward, backward, and bidirectional) using numerical models. They discovered that bidirectional pumping was a slightly superior option (Wang et al. 2022). In another study, Wang et al. adopted the bidirectional pumping scheme. They observed that the ASE evolution along the fiber was consistent with typical ASE variations under bidirectional pumping (Wang et al. 2024). Almukhtar et al. showed an innovative small hybrid broadband optical amplifier which consists of a mixture of Hafnium Bismuth Erbium co-doped (HB-EDF) and Zirconia-Yttria Aluminum co-doped erbium (Zr-EDF) using both as the gain medium. This was achieved by creating a structure which allows 1 m HB-EDF and 2 m of Zr-EDF to be utilized in either a single pass or double pass configuration respectively (Almukhtar et al. 2019). Mirza et al. proposed an efficient TDFA design for both booster and in-line use in double-hop ground-to-satellite optical wireless communication links based on a two-stage pumping scheme (Mirza et al. 2023). Fang et al. theoretically and experimentally confirmed that the balance optimization problem between high gain and low differential mode gain of a four-mode EDFA can be solved with a bidirectional hybrid mode pumping scheme compared to a conventional bidirectional hybrid mode pumping scheme (Fang et al. 2024). Ososkov et al. used a conventional bidirectional pumping scheme in their experiments to improve pump efficiency (Ososkov et al. 2021). Taengnoi et al. bidirectionally pumped bismuth-doped fiber (BDF) at two wavelengths (1240 nm and 1267 nm) to broaden and flatten the gain spectrum. The total pump power was determined to be 720 mW (Taengnoi et al. 2021). Śliwczyński et al. investigated a bidirectional fiber optic link consisting of two end terminals connected by a series of fiber lines and a bidirectional optical amplifier (Śliwczyński et al. 2019). Firstov et al. realized an experimental setup of a typical BDFA using a commercially available bidirectional pumping scheme (Firstov et al. 2016). Yücel and Dinçer compared three types of S-bands TDFA designs. The three different designs were a single-pass, a double-pass, and two-stage triple-pass (Yucel and Dincer 2022). Facchini et al. conducted an experimental and simulation study to measure the radiation response of two-stage optical amplifier through gain distortion, noise figure, and associated active fiber using an experimental-simulation approach due to radiation-induced attenuation (Facchini et al. 2025). Li et al. conducted both theoretical and experimental investigations into the gain and noise properties of low repetition rate pulsed double

pass amplifiers (Li et al. 2019). Lan et al. experimentally achieved a net Raman gain of approximately 15 dB over a bandwidth of approximately 2.1 THz in the U band under a distributed bidirectional Raman pump configuration (Lan et al. 2024). Ren et al. proposed a bidirectional pumped EDFA system using Optisystem software. İn this study, the gain characteristics of the EDFA were investigated considering pump power, fiber length, erbium concentration, and input signal power (Ren et al. 2023). Donodin et al. demonstrated an innovative bismuth-doped fiber amplifier for E-band applications, exhibiting unprecedented performance that includes the highest power conversion efficiency ever recorded for telecom compatible amplifiers in this band (Donodin et al. 2024). Wu et al. demonstrated approximately 18 kW output power level using a tandem-pumped bidirectionally pumped confined doped fibre amplifier (Wu et al. 2022). Elmouaddine et al. developed a seven-core erbium-doped double-layer fiber amplifier. They proposed bidirectional pumping to analyze the effect of a second pump on gain and NF (Elmouaddine et al. 2023). Mishra et al. proposed that they integrate the amplifier and optical band-pass filter into a singular unit that utilizes a narrow bandwidth (generally ~3nm or less depending on application) (Mishra et al. 2022). Huang et al. experimentally demonstrated a bidirectional, cross-gain-modulation-free BDFA for O-band high-speed passive optical networks (Huang et al. 2025). Ahmad et al. proposed and characterized a bidirectional depressed-cladding EDFA for continuous wave S-band operation (Ahmad et al. 2009). Awsaj et al. analyzed the gain and NF of an EDFA using a double-pass wave-selective coupler (Awsaj et al. 2021). Ma et al. reported an all-fiberized narrow-linewidth amplifier with a record 5 kW output power, utilizing a bidirectional pumping scheme within a main oscillator power amplification setup (Ma et al. 2021). Jamalus et al. demonstrated two-stage TDFAs using pump power distribution techniques. They utilized OptiSystem v.13 software to perform simulations with signal wavelengths ranging from 1975 nm to 2000 nm (Jamalus et al. 2029). Wang et al. optimized pump wavelengths to provide flat gain characteristics. Bismuth-doped phosphosilicate fibers were bidirectionally pumped employing a dual-wavelength pumping scheme with two laser diodes operating at 1270 nm and 1310 nm (Wang et al. 2023). Obaid et al. demonstrated the success of optical amplification across the S, L, and C bands. They proposed a hybrid amplifier using a combination of a bidirectional TDFA and a multi-section fiber optic parametric amplifier (Obaid et al. 2024).

The O-band, especially in applications requiring high speed and capacity, necessitates high-gain amplifiers to compensate for signal losses and increase transmission distance. This study examines the DP-PDFA configuration, presented for the first time in the literature as an alternative to the traditional BD-PDFA configuration, to meet this requirement. The fundamental components of the amplifier design PDF length, signal power, and pump power have been optimized with respect to gain. Furthermore, these parameters have been analyzed and compared with respect to both gain and NF.

Finally, BD-PDFA and DP-PDFA are analyzed with respect to the PCE and ASE noise power, respectively. It was observed that the DP-PDFA configuration system achieved significantly higher gain compared to the BD-PDFA configuration. In addition, care has been taken to ensure that the parameters determined within the scope of the study are within applicable ranges. When compared with the existing literature, it offers higher gain, greater efficiency, and commercially feasible DP-PDFA configuration models.

2. Theoretical Analysis

To design a high-efficiency PDFA in the O-band, an understanding of the theoretical background of PDFs is necessary. In this context, examining the energy level diagram, emission equations of PDFs, and emission and absorption cross-sections is of great importance. The emission and absorption cross-sections of Pr^{3+} are presented in Figure 1.

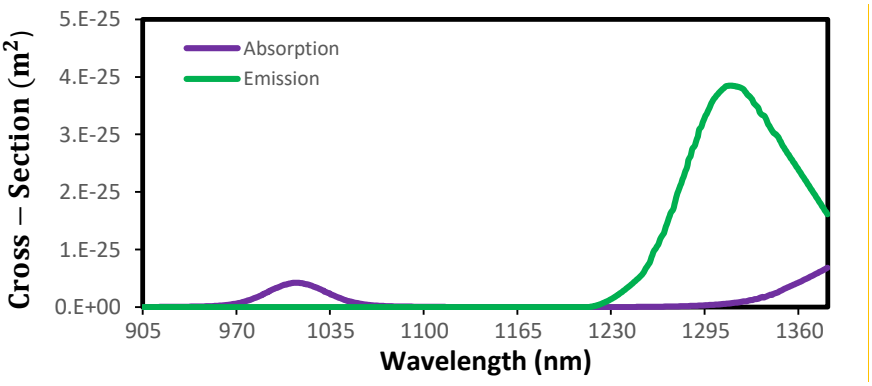


Figure 1. Emission and absorption cross-section spectra of Pr^{3+}.

The purple and green curves represent the ground state absorption (GSA) and emission of the Pr^{3+} ion, respectively. Although the Pr^{3+} ion exhibits two pump absorption bands centered at 1010 nm and 1400 nm, pump wavelengths between 1000 nm and 1040 nm are typically utilized for excitation. Furthermore, the emission cross-section peaks around 1300 nm (Mirza et al. 2021; Husein, and El-Nahal 2010; Schimmel et al. 2001; Ohishi et al. 1992; Morin and Taufflieb 1997). Generally, laser pumping schemes in doped fiber amplifiers are based on the absorption spectrum of the dopant ions (Mukhtar et al. 2020). A simplified five-level energy diagram of the Pr^{3+} ion is shown in Figure 2.

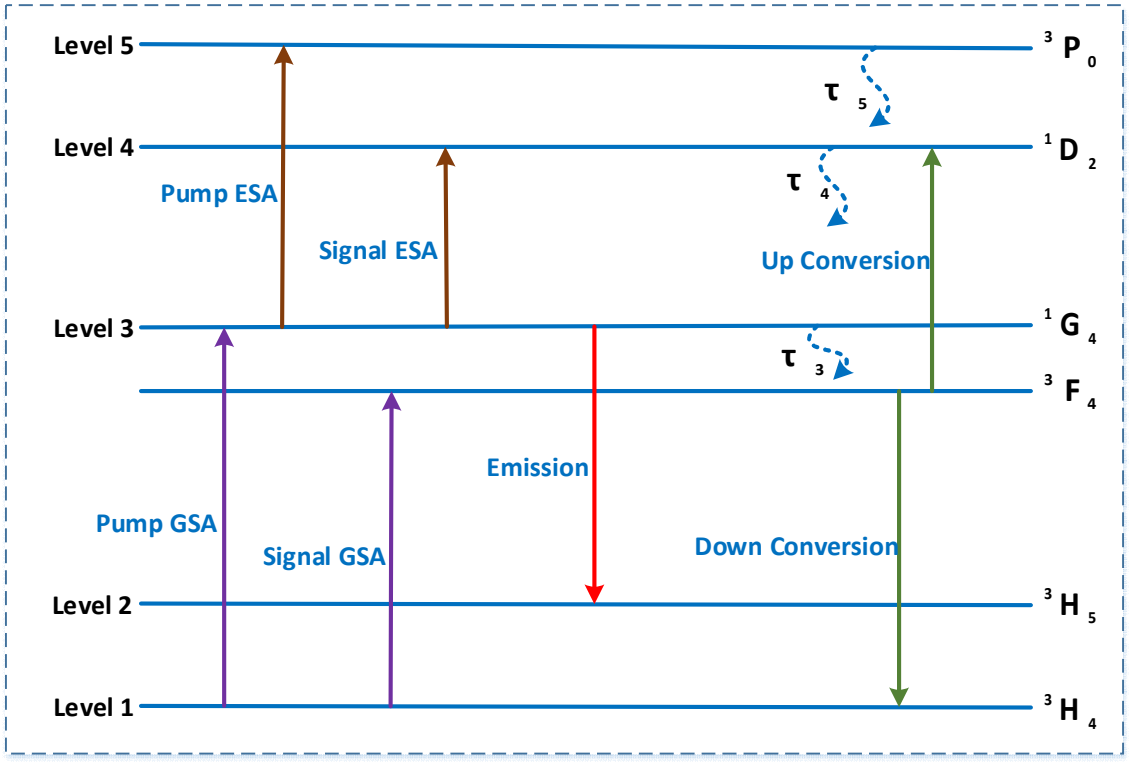


Figure 2. Five level energy diagram of Pr^{3+}.

The basic transitions between energy levels are identified as $^1G_4$, $^3P_0$, $^1D_2$, $^3F_4$, $^3F_3$, $^3H_5$ and $^3H_4$ (Optiwave). GSA and emission occur through the $^1G_4 \leftrightarrow {}^3H_4$ transitions. Signal absorption and signal emission are provided by the $^3H_4 \rightarrow {}^3F_4$ and $^1G_4 \rightarrow {}^3H_5$ transitions, respectively. Furthermore, the upconversion effect occurring through the $^1G_4 \rightarrow {}^1D_2$ and $^1G_4 \rightarrow {}^3H_5$ transitions can reduce the carrier density at the $^1G_4$ level (Berkdemir and Ozsoy 2007). This occurs because the energy difference between the $^1G_4$ and $^1D_2$ levels is equal to that between the $^1G_4$ and $^3H_5$ levels (Mirza et al. 2021; Berkdemir and Ozsoy 2007). Based on the energy diagram presented in Figure 2, the Pr^{3+} optical amplifier system can be modeled using the following rate equations (Ohishi et al.1992).

$$\frac{dN_3}{dt} = T_{13}N_1 - \left(T_{35}+T_{34}+T_{32}+T_{31}+\frac{1}{\tau_3}+cN_3\right)N_3 + \frac{B_{43}}{\tau_4}N_4 + \frac{B_{53}}{\tau_5}N_5 \quad (1)$$

$$\frac{dN_4}{dt} = \left(T_{35}+\frac{c}{2}N_3\right)N_3 - \frac{N_4}{\tau_4} \quad (2)$$

$$\frac{dN_5}{dt} = T_{35}N_3 - \frac{N_5}{\tau_5} \quad (3)$$

The transition rates T_{13}, T_{31}, T_{32}, T_{34}, and T_{35} in the equations above are expressed as $\frac{P_p\sigma_{13}\eta_p}{A_c h\nu_p}$, $\frac{P_p\sigma_{31}\eta_p}{A_c h\nu_p}$, $\frac{P_s\sigma_{32}\eta_s}{A_c h\nu_s}$, $\frac{P_s\sigma_{34}\eta_s}{A_c h\nu_s}$, and $\frac{P_s\sigma_{35}\eta_s}{A_c h\nu_s}$ respectively. The total ion density is given in equation (4).

$$N_t = N_1 + N_2 + N_3 + N_4 + N_5 \tag{4}$$

The transitions between the energy levels $^3H_4$ and $^1G_4$, expressed as N_1 and N_3 respectively, directly determine the gain of the PDFA. The ratio equation for a signal propagating in a PDFA gain medium with thickness *dz* can be written as follows, based on source (Khamis et al. 2018):

$$\frac{dP_s}{dz} = [N_3(T_{32} - T_{34}) - N_1 T_{13}] P_s \Gamma_s \tag{7}$$

The T_{34} in the equation above represents the ESA cross-section at the signal wavelength and has been ignored by the OptiSystem software. Accordingly, the calculated gain equation is presented as follows (Khamis et al. 2018).

$$G = \frac{P_s(L)}{P_s(0)} = exp([L\Gamma_s\{N_3(T_{32} - W_{34}) - N_1 T_{13}\}]) \tag{8}$$

A critical parameter in the characterization of optical amplifiers is the NF, which is conventionally expressed in decibels (dB) (Kweon 2002). Mathematically, it is defined as follows:

$$NF = 10log_{10}\frac{SNR_{in}}{SNR_{out}} \tag{9}$$

Table 1. The key symbols in equations (1)–(9)

Symbol	**Description of the Symbol**
N_1, N_2, N_3, N_4, N_5	Ion density at different levels
T_{ij}	The transition rates between energy levels *i* and *j*
τ_3, τ_4, τ_5	Spontaneous ion lifetimes of $^1G_4$, $^1D_2$, and $^3P_0$ levels
P_p, P_s	Pump and signal power
σ_{ij}	The stimulated emission cross-section between energy levels *i* and *j*
η_p, η_s	The fractional pump and signal powers within the PDF core
Γ_s	Overlapping integral of the signal
A_c	Doped fiber core area
c	Upconversion coefficient
L	PDF length
h	Planck constant
ν_s, ν_p	Signal and pump frequencies
N_t	Total ion density
SNR_{in}, SNR_{out}	Input and output signal to noise ratio

3. Simulation Setup

System schematics for the BD-PDFA and DP-PDFA configurations are shown in Figure 3. In Figure 3(a), signals applied with a TLS are combined with pump laser 1 at pump coupler 1 and pump laser 2 at pump coupler 2 and then applied to the PDF. The amplified signals are then directed to the optical spectrum analyzer (OSA) for measurement, thereby completing the BD-PDFA configuration.

In Figure 3(b), signals applied with a tunable laser source (TLS) enter from terminal 1 and exit from terminal 2 of the optical circulator, are combined with the pump laser at the pump coupler and then applied to the PDF. The amplified signal reflects off the reflector, passes through the PDF again, enters terminal 2 of the circulator, and exits from terminal 3. The amplified signals are then directed to the OSA for measurement, thereby completing the DP-PDFA configuration.

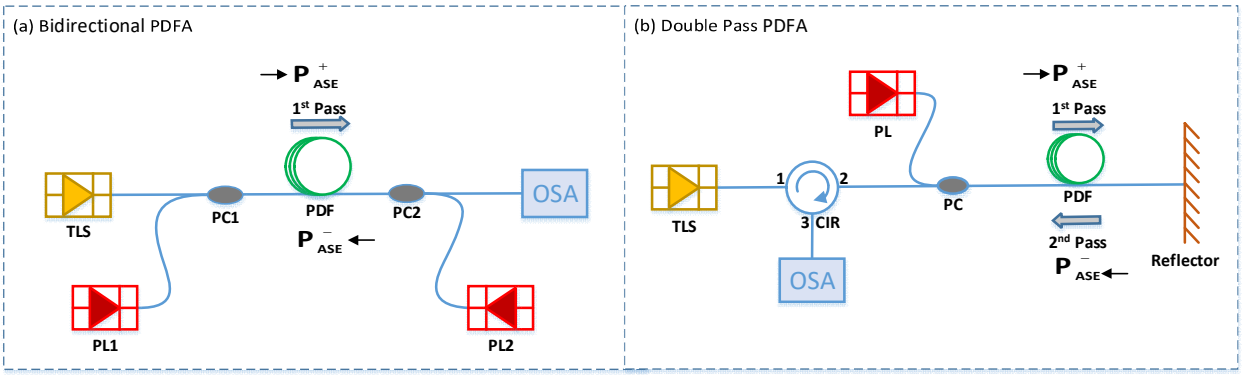


Figure 3. Configuration setups for (a) BD-PDFA and (b) DP-PDFA. TLS: Tunable Laser Source, PC: Pump Coupler, PL: Pump Laser, PDF: Pr^{3+} Doped Fiber, P_{ASE}^{+} and P_{ASE}^{-}: forward and backward propagating ASE: CIR: Circulator

OSA was used to observe and analyze the results. PDF length, signal power, pump power, and input signal wavelength are the main important parameters for PDFA analyses. Therefore, they were determined to analyze and compare the two amplifiers.

Firstly, the initial values determined in the Optisystem software were used, as shown in Table 2. For the O band, the peak performance signal wavelength located at 1310 nm was selected for PDF length, signal power, and pump power parameter analyses. The initial value for the pump wavelength was selected as 1020 nm.

Because optical amplifiers are generally preferred in communication applications, single-mode fibers are used in this study. Because the system design is carried out independently of polarization, polarization effects were not taken into account. In all simulations, the additional loss value was fixed at 0,02 dB.

The main parameters determined in Table 2 are the initial parameters assigned by the simulation. Furthermore, these parameter values are consistent with parameters analyzed experimentally and

in simulations in the literature. Each analyzed parameter range is equal for both PDFA configurations.

The system parameters were optimized employing the single parameter optimization (SPO) method. Starting with the values determined in Table 2, the optimum values of the most important main parameters for PDFA amplifier design, namely PDF length, signal power, and pump power, were determined with respect to gain. Each parameter was optimized consecutively based on preceding results, evaluating the system performance with respect to gain and NF at every stage. Then, the gain spectrum for the 1270–1340 nm band range was re-analyzed with respect to gain and NF.

Each parameter analysis was primarily evaluated with respect to gain and NF. Then, it was analyzed with respect to PCE and ASE noise power analyses, respectively. In all the graphs obtained as a result of optimization, the triangular dotted represent BD-PDFA simulation results, and the circular lines represent DP-PDFA simulation results. Blue results represent gain, and red results represent NF.

Table 2: Initial values of the primary simulation parameters

Parametre	Initial values	Analysis Range	Step Range İncrease
Signal Wavelength (nm)	1310	1270 – 1340	5
PDF Length (m)	5	1 – 24	1
Signal Power (dBm)	0	0 – (-50)	-5
Total Pump Power (mW)	100	100 – 1200	100
Upconversion (m^3/s)	$0{,}2x10^{-21}$	None	None
Ion Density (m^{-3})	$10x10^{24}$	None	None
Numerical Aperture	0,364	None	None
Doping Radius (um)	1	None	None
Core Radius (um)	1	None	None
Pump Wavelength (nm)	1020	None	None
Temperature (K)	300	None	None

4. Result and Discussion

Optimizing the signal power, PDF length, and pump power is essential for an effective PDFA design. Furthermore, a comparative analysis of BD-PDFA and DP-PDFA configurations is essential for selecting the best option with respect to cost and performance. Optimizing the amplifier configurations with respect to gain requires optimizing the PDF length, signal power, and pump power. After obtaining the optimum values for the determined parameters, it is

important to analyze and compare the gain and NF of the 1270-1340 band range for the both amplifier configurations. SPO method was used to optimize the determined parameters. The flowchart of the optimization algorithm is shown in Figure 4.

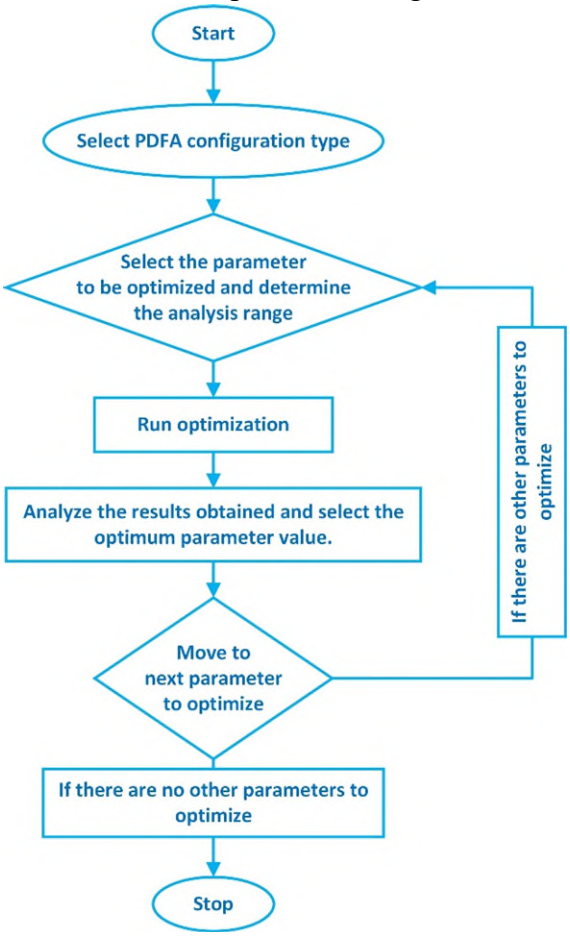


Figure 4. Flow chart of the optimization algorithm.

Initially, the values in Table 2 were determined, and the parameter range for different PDF size analyses was increased from 1 to 24 m in increments of 1 m. The results obtained are shown in Figure 5. Here, increasing the PDF size initially caused an increase in amplifier gain, but as it continued to increase, the amplifier reached saturation and subsequently decreased in gain. Optimum PDF lengths were obtained for BD-PDFA and DP-PDFA at approximately 10 m and 5 m, respectively. For BD-PDFA, an amplifier gain of 11,09 dB was obtained at a PDF size of 10 m. For DP-PDFA, an amplifier gain of 14,26 dB was obtained at a PDF size of 5 m. When NF was examined, it was approximately 3,91 dB on average for BD-PDFA and approximately 5,26 dB for DP-PDFA. With respect to gain, DP-PDFA performed better and was optimum when the PDF size was 5 m shorter. With respect to NF, BD-PDFA performed better.

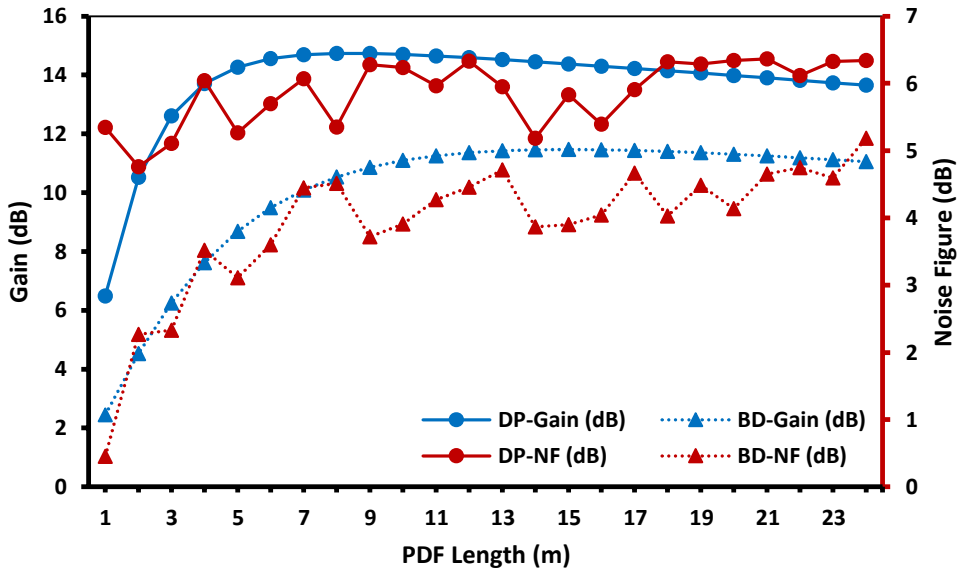


Figure 5. Change of gain and NF depending on different PDF lengths.

Figure 6 shows how changes in signal power affect the gain and NF. Signal power was increased in the range of 0 – (-50) dBm and -5dBm steps. Initially, increasing signal power increased the gain in the amplifiers, but as the increase continued, the amplifiers reached saturation and subsequently decreased in gain. Examining Figure 6, it can be seen that BD-PDFA saturates faster. Optimum signal power were obtained for BD-PDFA and DP-PDFA at -20 dBm and -30 dBm, respectively. For BD-PDFA, the amplifier gain was 14.51 dB at -20 dBm, and for DP-PDFA, the amplifier gain was 26.36 dB at -30 dBm. With respect to NF, while BD-PDFA initially had a lower NF, it increased significantly as the signal power increased. DP-PDFA's NF was initially higher than BD-PDFA's, but remained more stable as the signal power increased. As signal power increases, the NF of DP-PDFA becomes lower than that of BD-PDFA.

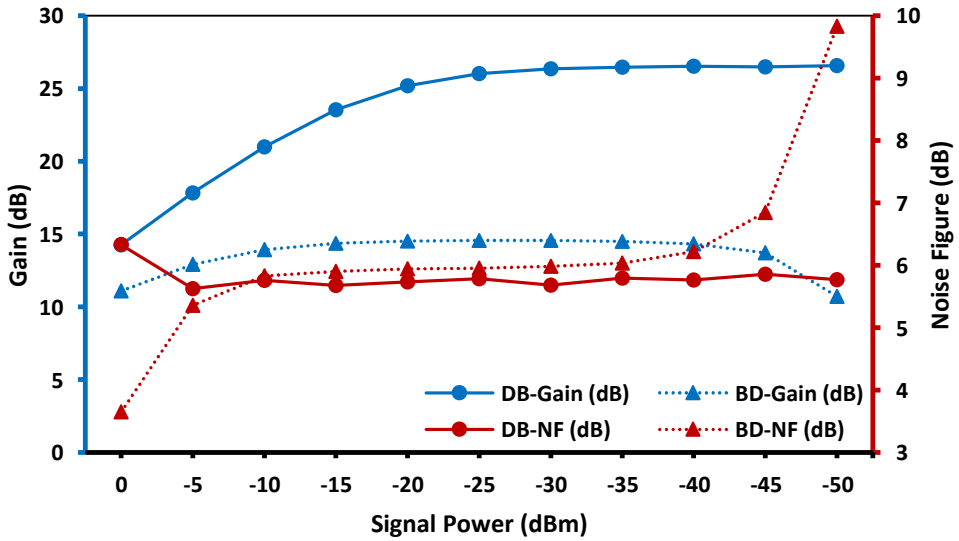


Figure 6. Change of gain and NF depending on different signal powers.

Figure 7 shows how changes in pump power affect the gain and NF. The total pump power was increased in the range of 100 – 1200 mW in 100 mW step increments. When the total pump power reached 800 mW for both amplifier configurations, the efficiency on gain began to decrease. Optimum total pump power was obtained at 800 mW for BD-PDFA and DP-PDFA. For BD-PDFA and DP-PDFA, gains of 41,39 dB and 47,42 dB were obtained at 800 mW. The NF was obtained on average as 5,53 dB and 5,65 dB for BD-PDFA and DP-PDFA, respectively. With respect to gain, the DP-PDFA system performed 6 dB better than the BD-PDFA system. With respect to NF, the two amplifiers obtained similar NF values for 800 mW pump power.

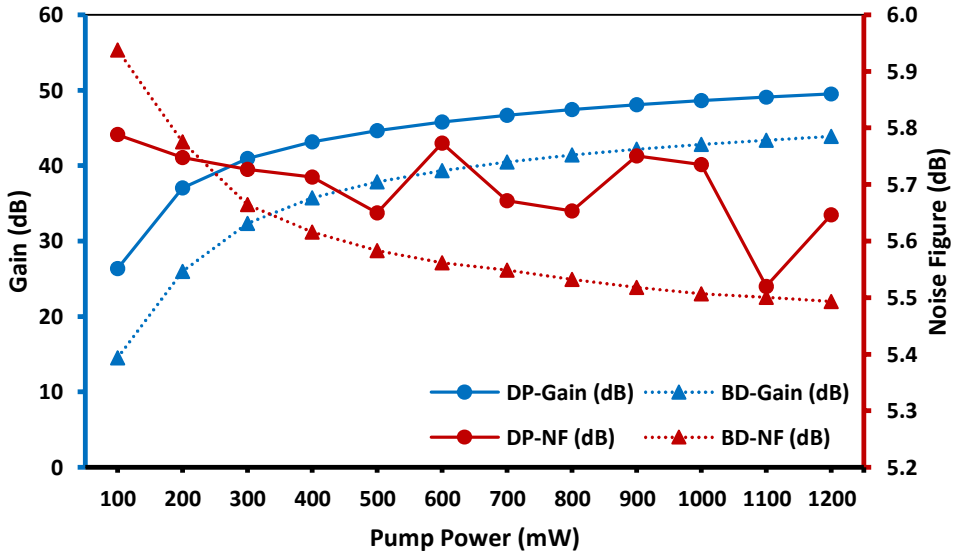


Figure 7. Change of gain and NF depending on different pump powers.

After determining the optimum values of the TLS signal power, PDF length, and pump laser power parameters, the 1270-1340 band range for the O Band was analyzed with respect to gain and NF for both amplifier configurations. The results obtained are shown in Figure 8. It is observed that the gains are maximum around 1310 nm for both amplifiers. Although the gains of the two amplifiers were initially close, the signal power around 1310 nm showed that the DP-PDFA system performed much better than the BD-PDFA system. When looking at NF, it was observed that it was initially low for both amplifiers but increased as the signal wavelength increased. While the DP-PDFA had a higher NF initially, the increase in NF as the signal power increased was less than that of the BD-PDFA.

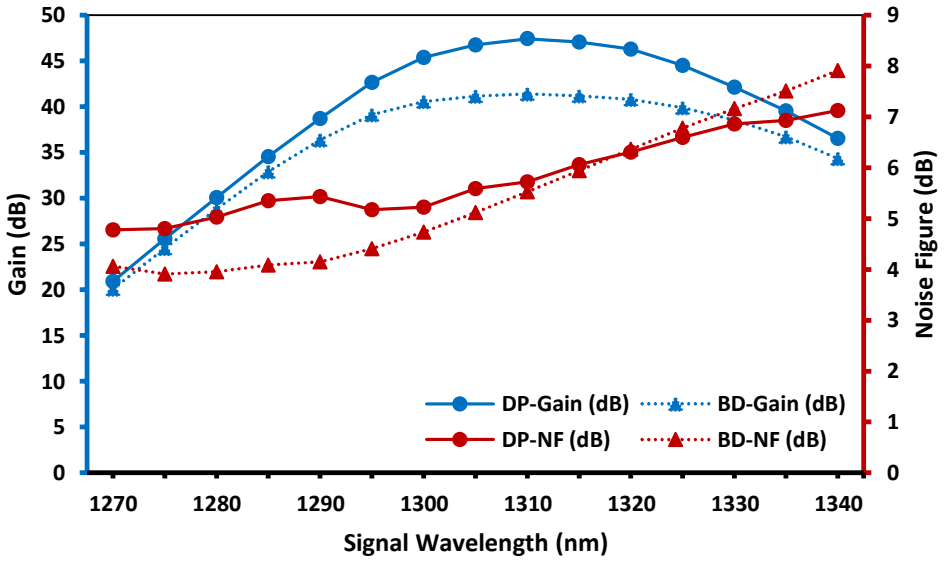


Figure 8. Change of gain and NF depending on different signal wavelengths.

Table 3 compares the effects of PDF size and signal power change on gain and NF performance for two amplifiers. The optimized values in Table 5 were set the same for both amplifiers, and combinations of optimal PDF length and signal power values were tested to accurately compare their performance. As can be seen from Table 3, in every combination, the DP-PDFA system shows a significant gain difference and performs better than the BD-PDFA system. With respect to NF, although BD-PDFA has less NF, the values are quite close to each other.

Tablo 3: Performance trade-offs of the amplifier configurations

PDF Length (m)	Signal Power (dBm)	Double Pass		Bidirectional	
		Gain (dB)	NF (dB)	Gain (dB)	NF (dB)
10	-20	44,5	6,0	41,4	5,5
10	-30	49,8	5,9	45,6	5,5
5	-20	42,8	5,8	29,1	5,6
5	-30	47,4	5,7	29,4	5,7

The pump laser enables efficient stimulated emission and signal amplification by providing a continuous population inversion among praseodymium ions. The output power and operating efficiency of the pump laser have a direct determining effect on the gain characteristic and signal amplification performance of the PDFA. An optimally designed pumping system ensures that signal gain is maximized while keeping NF at a minimum level.

The PCE parameter, which represents the efficiency of converting pump power into signal power, was calculated in this study. The term PCE is frequently used in optical amplifiers instead of the

concept of laser efficiency. PCE, which is used in the quantitative analysis of the efficiency of converting pump power to optical gain, is mathematically defined as follows (Wang et al. 2022):

$$PCE(\%) = \frac{P_{s_{out}} - P_{s_{in}}}{P_p} \quad (10)$$

Where $P_{s_{in}}$, $P_{s_{out}}$, and P_p represent the input signal power, the amplified signal power, and the pump power, respectively. The PCE for both amplifier configurations was calculated utilizing the optimized parameters detailed in Table 5. The resulting PCE values were determined to be 42.6% for the BD-PDFA and 63.3% for the DP-PDFA. Finally, Table 4 presents a performance comparison between the proposed current study and existing literature.

Table 4: Comparison with the Literature.

Study	**(Alharbi et al. 2022)**	**(Khan et al. 2024)**	**(Mohammed et al. 2022)**	**Current Study**	**Current Study (Proposed)**
Design Type	Bidirectional Single Pass PDFA	Bidirectional Single Pass PDFA	Two Stage Double Pass PDFA	Bidirectional Single Pass PDFA	One Stage Double Pass PDFA
Signal Wavelength (nm)	1310	1312	1300	1310	1310
PDF Length of each stage (m)	15	27	1,5	10	5
Signal Power (dBm)	0	-30	-10	-20	-30
Total Pump Power (mW)	3000	700	700	800	800
Upconversion (m^3/s)	0	-	-	$0{,}2x10^{-21}$	$0{,}2x10^{-21}$
Ion Density (m^{-3})	$50x10^{24}$	$3x10^{24}$	$50x10^{24}$	$10x10^{24}$	$10x10^{24}$
Numerical Aperture	0,34	0.38	-	0,36	0,36
Doping Radius (μm)	0,8	1	-	1	1
Core Radius (μm)	1,2	1	1	1	1
Pump Wavelength (nm)	1030	1017	1030	1020	1020
Temperature (K)	300	-	-	300	300
PCE (%)	47	-	14	42,6	63,3
Gain (dB)	56,4	44.56	34,6	41,39	47,42
Noise Figure (dB)	4,1	4.1 (min.)	5,8 (min.)	5,53	5,65

Using the optimum parameter values specified in Table 4, the change of the ASE noise power with signal wavelength for both amplifier systems is shown in Figure 10. Simulations for both amplifier systems were performed in the Optisystem software environment using a resolution bandwidth of 0.01 nm. At a signal wavelength of 1310 nm, the ASE power was measured as -20,2 dBm for BD-PDFA and -12,2 dBm for DP-PDFA.

ASE propagates in both forward and backward directions within the gain medium. The forward propagating ASE component and the backward propagating ASE component are stated by P_{ASE}^{+} and P_{ASE}^{-}, respectively. In a bidirectional PDFA configuration, pump power propagates through the gain medium in both forward and reverse directions, simultaneously initiating stimulated

emission processes throughout the active region. This results in the formation of ASE components in both directions and their mutual amplification. Bidirectional accumulation of ASE generates additional photon density in the gain medium, forcing part of the pump to be used to amplify unwanted ASE signals. As a result, the pump power cannot effectively contribute to signal gain, reducing the overall gain of the system. In contrast, in a DP-PDFA configuration, because pump and signal propagation are limited to a specific direction, ASE accumulation is more controlled, and pump energy is more effectively converted to signal gain. Consequently, BD-PDFA systems have higher ASE noise power and lower gain compared to DP-PDFA systems due to the increased ASE noise power and decreased pump efficiency.

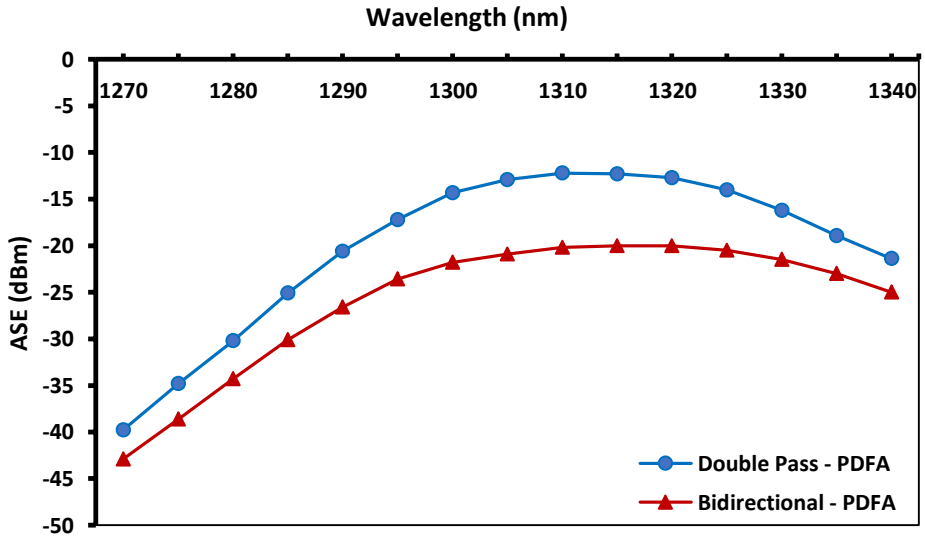


Figure 10. ASE noise power variation as a function of signal wavelength.

A comparison of the BD-PDFA and DP-PDFA configurations for practical applications reveals similar results with respect to gain and NF. Since this study prioritizes practical applicability, both amplifier configurations are considered suitable options for real-world system designs. The DP-PDFA configuration offers higher gain compared to the BD-PDFA, while the BD-PDFA configuration stands out with its lower NF. However, when evaluated with respect to PDF length, number of pumps, and PCE, the DP-PDFA configuration is determined to be more advantageous. On the other hand, while DP-PDFA systems require the use of additional passive components such as circulators and reflectors, BD-PDFA configurations require additional hardware such as pump couplers, PDF length controllers, pump lasers, laser current drivers, and temperature drivers. The high cost of pump lasers, in particular, makes the DP-PDFA configuration more cost-effective. Furthermore, the DP-PDFA configuration exhibits higher performance with respect to PDF length, gain, and PCE. Since the gain parameter generally plays a decisive role in optical systems, it was concluded that the DP-PDFA configuration is a more suitable option for practical designs.

CONCLUSION

Analyzing new configurations of PDFAs that could be an alternative to EDFAs is quite important. Upon reviewing the literature, the proposed DP-PDFA system was simulated for the first time.

The DP-PDFA system was compared with the traditional BD-PDFA system and found to perform significantly better. For both amplifiers, the PDF length, signal power, and pump power were analyzed comparatively with respect to gain and NF. For the second window, the O band, the gain and NF in the 1270-1340 nm signal wavelength range were also analyzed. The optimized parameters and the resulting values for both amplifier configurations are shown comparatively in Table 5.

Table 5: Optimized parameter values and the results obtained from these values.

Parameter	Bidirectional PDFA	Double-Pass PDFA
Signal Wavelength (nm)	1310	1310
PDF Length (m)	10	5
Signal Power (dBm)	-20	-30
Total Pump Power (mW)	800	800
PCE (%)	42,6	63,3
Gain (dB)	41,39	47,42
Noise Figure (dB)	5,53	5,65

As a result of parameter optimizations, the maximum gain obtained for the BD-PDFA structure was approximately 41.39 dB and NF was 5.53 dB. In the DP-PDFA configuration, these values were obtained as a maximum gain of 47.42 dB and NF of approximately 5.65 dB. In the comparison made with a reference signal wavelength of 1310 nm, DP-PDFA showed approximately 6 dB better performance with respect to gain compared to BD-PDFA. The NF values were observed to be close for both amplifiers. When examined from a design perspective, it was determined that the proposed DP-PDFA system is significantly more efficient, and this shows that preferring the DP-PDFA system instead of BD-PDFA would be a more suitable approach. The obtained results provide a fundamental reference for optical amplifier manufacturers and researchers in system design and optimization processes.

REFERENCES

Kanwal, B., Armghan, A., Ghafoor, S., Atieh, A., Sajid, M., Kausar, T., ... Lu, Y.: Design and analysis of an O+ E-band hybrid optical amplifier for CWDM systems. Micromachines 13(11), 1962 (2022). https://doi.org/10.3390/mi13111962

Winzer, P.J., Neilson, D.T., Chraplyvy, A.R.: Fiber-optic transmission and networking: the previous 20 and the next 20 years. Optics Express 26(18), 24190–24239 (2018). https://doi.org/10.1364/OE.26.024190

Ferrari, A., Napoli, A., Fischer, J.K., da Costa, N.M.S., D'Amico, A., Pedro, J., ... Stavdas, A.: Assessment on the achievable throughput of multi-band ITU-T G. 652.D fiber transmission systems. Journal of Lightwave Technology 38(16), 4279–4291 (2020)

Mirza, J., Imtiaz, W.A., Aljohani, A.J., Atieh, A., Ghafoor, S.: Design and analysis of a 32x5 Gbps passive optical network employing FSO based protection at the distribution level. Alexandria Engineering Journal 59(6), 4621–4631 (2020). https://doi.org/10.1016/j.aej.2020.08.020

Chen, Y., Li, J., Zhou, P., Zhu, P., Tian, Y., Wu, Z., Zhu, J., Liu, K., Ge, D., Chen, J.: MDM-TDM PON utilizing self-coherent detection-based OLT and RSOA-based ONU for high power budget. IEEE Photonics Journal 8(3), 1–7 (2016)

Krishna Sarma, K.V.S., Khan, M.M.: Design, optimization, and evaluation of ultra-broadband hybrid optical doped-fiber amplifier for O+E+S+C band amplification. Optik 329, 172328 (2025). https://doi.org/10.1016/j.ijleo.2025.172328

Elson, D.J., Wakayama, Y., Mikhailov, V., Luo, J., Yoshikane, N., Inniss, D., Tsuritani, T.: 9.6-THz single fibre amplifier O-band coherent DWDM transmission. Journal of Lightwave Technology 42(4), 1203–1208 (2024). https://doi.org/10.1109/JLT.2024.3354083

Ferrari, A., Virgillito, E., Curri, V.: Band-division vs. space-division multiplexing: A network performance statistical assessment. Journal of Lightwave Technology 38(5), 1041–1049 (2020)

Hui, R.: Introduction to fiber-optic communications. Academic Press (2019)

Rapp, L., Eiselt, M.: Optical amplifiers for multi–band optical transmission systems. Journal of Lightwave Technology 40(6), 1579–1589 (2021)

Luo, Y., Wen, J., Zhang, J., Canning, J., Peng, G.-D.: Bismuth and erbium codoped optical fiber with ultrabroadband luminescence across O, E, S, C, and L-bands. Optics Letters 37(16), 3447–3449 (2012). https://doi.org/10.1364/OL.37.003447

Mirza, J., Ghafoor, S., Habib, N., Kanwal, F., Qureshi, K.K.: Performance evaluation of praseodymium doped fiber amplifiers. Optical Review 28(6), 611–618 (2021)

ThorLabs.: O-Band fiber amplifiers (PDFAs). https://www.thorlabs.com/newgrouppage9.cfm?objectgroup_id=12403 (2025)

Fiberlabs Inc.: O-band PDFA Bench-top. https://www.fiberlabs.com/products/product_details/o-band-pdfa-bench-top/

Alharbi, A.G., Mirza, J., Raza, M., Ghafoor, S.: Performance enhancement of praseodymium doped fiber amplifiers. Computers, Materials & Continua 73(3), 5411–5422 (2022). https://doi.org/10.32604/cmc.2022.029317

Cumberland, B., Ferin, A., Rulkov, A.B., Travers, J.C., Popov, S.V., Taylor, J.R.: Fiber lasers in IR, VIS and UV. In: Fiber Lasers IV: Technology, Systems, and Applications, Proc. SPIE 6453, 64530A (2007). https://doi.org/10.1117/12.706466

Webber, T.: Advances in fiber lasers for the materials processing market. In: Conference on Lasers and Electro Optics 2012, OSA Technical Digest (2012). https://doi.org/10.1364/CLEO_AT.2012.JTh4I.4

He, B., Lou, Q., Zhou, J., Dong, J., Wei, Y., Xue, D., Qi, Y., Su, Z., Li, L., Zhang, F.: High power coherent beam combination from two fiber lasers. Optics Express 14(7), 2721–2726 (2006). https://doi.org/10.1364/OE.14.002721

Maharry, A., Liu, J., Misak, S., Andrade, H., Valenzuela, L.A., Gilardi, G.: First demonstration of an O-band coherent link for intra data center applications. Journal of Lightwave Technology 41(21), 6643–6650 (2023). https://doi.org/10.1109/JLT.2023.3290487

Obaid, H.M., Shahid, H., Akram, A., Zafrullah, M.: Performance optimization of dual-stage and bidirectional pumped thulium-doped fiber amplifier configuration for improved gain using multiparameter optimization algorithm. Optical and Quantum Electronics 56, 1085 (2024). https://doi.org/10.1007/s11082-024-07062-7

Wu, Y., Wang, Z., Xie, Z., Ji, J., Wang, K.: Numerical simulation of thulium-doped fiber amplifier at 2 μm. Optoelectronics Letters 21(10), 582–588 (2025). https://doi.org/10.1007/s11801-025-4138-1

Ali, A.Y., Al-Mashhadani, M.K.S., Al-Mashhadani, T.F., Awsaj, M.K., Bouteraa, Y.: Broadband flat amplification based on fully double-pass configuration in serial hybrid fiber amplifier. Optical and Quantum Electronics 54, 813 (2022). https://doi.org/10.1007/s11082-022-04245-y

Gurkaynak, I.A., Al-Mashhadani, M.K.S., Ali, M.H., Al-Mashhadani, T.F., Gunduz, A.E., Yucel, M., Goktas, H.H.: Widely flatness gain bandwidth with double pass parallel hybrid fiber amplifier. Optical and Quantum Electronics 53, 359 (2021). https://doi.org/10.1007/s11082-021-03021-8

Ali, M.H., Abdullah, F., Al-Mashhadani, T.F.: Gain-control technique in double-pass parallel hybrid fiber amplifier. Optical and Quantum Electronics 52, 386 (2020). https://doi.org/10.1007/s11082-020-02508-0

Khan, M.M., Gurjar, N.S.: Pump and signal optimization in thulium doped fiber amplifiers for S–band with amplified spontaneous emission and ion-ion interactions. In: 2022 IEEE 9th Uttar Pradesh Section International Conference on Electrical, Electronics and Computer Engineering (UPCON), pp. 1–6. IEEE (2022). https://doi.org/10.1109/UPCON56432.2022.9986482

Mirza, J., Ghafoor, S., Armghan, A., Elhamrawy, O.I., Jamal, L., Magam, M., Sheikh, S.I.M., Qureshi, K.K.: Performance enhancement of ytterbium-doped fiber amplifier employing a dual-stage in-band asymmetrical pumping. Micromachines 13(9), 1488 (2022). https://doi.org/10.3390/mi13091488

Wang, D., Pei, L., Zheng, J., Wang, J., Xu, W., Ning, T., Li, J., Wang, L.: Analysis of gain and noise characteristics of O-band Bi-doped fiber amplifier under different pumping schemes. Optik 251, 168491 (2022). https://doi.org/10.1016/j.ijleo.2021.168491

Wang, D., Pei, L., Zheng, J., Wang, J., Xu, W., Li, J., Ning, T.: Modeling optimization design and amplification characteristics of O-band irregular Bragg bismuth-doped fiber amplifier. Results in Physics 63, 107860 (2024). https://doi.org/10.1016/j.rinp.2024.107860

Almukhtar, A.A., Al-Azzawi, A.A., Ahmad, B.A., Cheng, X.S., Reddy, P.H., Dhar, A., Paul, M.C., Ahmad, H., Harun, S.W.: Flat-gain and wide-band partial double-pass erbium co-doped fiber amplifier with hybrid gain medium. Optik 178, 256–261 (2019). https://doi.org/10.1016/j.yofte.2019.101952

Mirza, J., Atieh, A., Menhas, M.I., Ghafoor, S., Magam, M., Jamal, L., Sheikh, S.I.M., Qureshi, K.K.: Design of an efficient thulium-doped fiber amplifier for dual-hop earth to satellite optical wireless links. Ain Shams Engineering Journal 14(7), 101983 (2023). https://doi.org/10.1016/j.asej.2022.101983

Fang, Y., Zhang, C., Zeng, Y., Xu, O., Huang, X., Zhang, X., Li, J., Fu, S., Qin, Y.: Simultaneous realization of high gain and low DMG of four-mode EDFA under bidirectional hybrid-mode pump. Optics Express 32(6), 9332–9342 (2024). https://doi.org/10.1364/OE.507023

Ososkov, Y., Khegai, A., Firstov, S., Riumkin, K., Alyshev, S., Kharakhordin, A., Lobanov, A., Guryanov, A., Melkumov, M.: Pump-efficient flattop O+E-bands bismuth-doped fiber amplifier with 116 nm –3 dB gain bandwidth. Optics Express 29(26), 44138–44145 (2021). https://doi.org/10.1364/OE.441775

Taengnoi, N., Bottrill, K.R.H., Hong, Y., Wang, Y., Thipparapu, N.K., Sahu, J.K., Petropoulos, P., Richardson, D.J.: Experimental characterization of an O-band bismuth-doped fiber amplifier. Optics Express 29(10), 15345–15355 (2021). https://doi.org/10.1364/OE.420995

Śliwczyński, Ł., Krehlik, P., Salwik, K.: Modeling and optimization of bidirectional fiber-optic links for time and frequency transfer. IEEE Transactions on Ultrasonics, Ferroelectrics, and Frequency Control 66(3), 632–642 (2019). https://doi.org/10.1109/TUFFC.2018.2889186

Firstov, S.V., Alyshev, S.V., Riumkin, K.E., Khopin, V.F., Guryanov, A.N., Melkumov, M.A., Dianov, E.M.: A 23-dB bismuth-doped optical fiber amplifier for a 1700-nm band. Scientific Reports 6, 28939 (2016). https://doi.org/10.1038/srep28939

Yucel, M., Dincer, A.: The gain and noise figure comparison of single-pass, double-pass, and dual-stage triple-pass thulium-doped fiber amplifiers in S-band with thulium-doped fiber optimization. Microwave and Optical Technology Letters 64(10), 1832–1840 (2022). https://doi.org/10.1002/mop.33364

Facchini, A., Morana, A., Boukenter, A., Mescia, L., Marin, E., Ouerdane, Y., Girard, S., Robin, T.: Investigation of the radiation response of a dual-stage optical amplifier. IEEE Transactions on Nuclear Science 72(8), 2774–2782 (2025). https://doi.org/10.1109/TNS.2025.3545269

Li, R., Fan, W., Wang, X., Li, X.: Improvement of noise and gain characteristics of low-repetition-rate double-pass fiber amplifiers. IEEE Photonics Journal 11(3), 7101710 (2019). https://doi.org/10.1109/JPHOT.2019.2909534

Lan, T., Xiang, J., Zhou, G., Xiang, M., Fu, S., Qin, Y.: Inverse design of incoherent Raman pump sources for U-band WDM transmission over 125 km G.652.D fiber. IEEE Photonics Journal 16(5), 7202106 (2024). https://doi.org/10.1109/JPHOT.2024.3453870

Ren, L., Pan, Y., Cheng, Y., Fu, Y., Bao, S., Yuan, L.: Gain simulation of bidirectional pumped broadband EDFA. In: 2023 Cross Strait Radio Science and Wireless Technology Conference (CSRSWTC), pp. 1–3 (2023). https://doi.org/10.1109/CSRSWTC60855.2023.10427508

Donodin, A., Manuylovich, E., Dvoyrin, V., Melkumov, M., Mashinsky, V., Turitsyn, S.: E-band telecom-compatible 40 dB gain high-power bismuth doped fiber amplifier with record power conversion efficiency. APL Photonics 9(4), 046102 (2024). https://doi.org/10.1063/5.0187069

Wu, H., Li, R., Xiao, H., Huang, L., Yang, H., Leng, J., Pan, Z., Zhou, P.: First demonstration of a bidirectional tandem-pumped high-brightness 8 kW level confined-doped fiber amplifier. Journal of Lightwave Technology 40(16), 5673–5681 (2022). https://doi.org/10.1109/JLT.2022.3183381

Elmouaddine, M., Nassiri, A., Boulezhar, A., Taibi, M.: Erbium doped seven-core fiber amplifier with bi-directional pumping. Nonlinear Optics, Quantum Optics 60, 123–135 (2023)

Mishra, A.R., Kakade, R.N., Kakade, P.D.: Dual-stage EDFA for improving the performance of long-haul optical systems. IEEE Access 10, 14193–14202 (2022). https://doi.org/10.1109/ACCESS.2022.3146978

Huang, Y., Huang, H., Vijayan, K., Wen, J., Borkowski, R., Fontaine, N.K., Chen, H., Iannone, P., Song, Y., Wang, T.: Bismuth-doped bidirectional fiber amplifier for high-speed passive optical networks. Journal of Lightwave Technology 43(13), 6361–6367 (2025). https://doi.org/10.1109/JLT.2025.3546506

Ahmad, H., Zulkifli, M.Z., Latif, A.A., Thambiratnam, K., Harun, S.W.: Bidirectional S–band continuous wave operation in a depressed-cladding erbium doped fiber amplifier. Journal of Optoelectronics and Advanced Materials 11(5), 547–553 (2009)

Awsaj, M.K., Goktas, H.H., Yucel, M., Awsaj, M.K.: Gain and noise figure analysis of erbium doped fiber amplifier based on double pass configuration using forward pumping. IOP Conference Series: Materials Science and Engineering 1094(1), 012095 (2021). https://doi.org/10.1088/1757-899X/1094/1/012095

Ma, P., Xiao, H., Liu, W., Zhang, H., Wang, X., Leng, J., Zhou, P.: All-fiberized and narrow-linewidth 5 kW power-level fiber amplifier based on a bidirectional pumping configuration. High Power Laser Science and Engineering 9, e45 (2021). https://doi.org/10.1017/hpl.2021.32

Jamalus, M.S.K.B., Yusoff, N.M., Sulaiman, A.H.: Simulation of dual stage thulium-doped fiber amplifier using pump power distribution technique. Indonesian Journal of Electrical Engineering and Computer Science 15(3), 1203–1211 (2019). http://doi.org/10.11591/ijeecs.v15.i3.pp1203-1211

Wang, Y., Wang, S., Halder, A., Sahu, J.: Bi-doped optical fibers and fiber amplifiers. Optical Materials: X 17, 100219 (2023). https://doi.org/10.1016/j.omx.2022.100219

Obaid, H.M., Rashid, F., Shahid, H., Khan, B., Zafrullah, M.: Gain flattened S+C+L-band bidirectional thulium doped fiber/ multi-section fiber optical parametric hybrid amplifier. Ain Shams Engineering Journal 15(1), 102497 (2024). https://doi.org/10.1016/j.asej.2023.102497

Husein, A.K.M., El-Nahal, F.I.: Noise figure and gain temperature dependent of Praseodymiumdoped fiber amplifier by using rate equations. Optics Communications 283(3), 409–413 (2010). https://doi.org/10.1016/j.optcom.2009.10.005

Schimmel, R.C., van de Sluis, H.J.D., Jonker, R.J.W., de Waardt, H.: Characterisation and modelling of Praseodymium doped fibre amplifiers. In: Proc. of IEEE/LEOS, Brussels, Belgium, Benelux Chapter, pp. 133–136 (2001)

Ohishi, Y., Kanamori, T., Tishi, T., Takahashi, S., Snitzer, E.: Concentration effect on gain of Pr3+-doped Fluoride fiber for 1.3 μm amplification. IEEE Photonics Technology Letters 4(12), 1338–1341 (1992)

Morin, V., Taufflieb, E.: High output-power Praseodymium doped fiber amplifier single pumped at 1030 nm: Analysis and results. IEEE Journal of Selected Topics in Quantum Electronics 3(4), 1112–1118 (1997)

Mukhtar, S., Aliyu, K.N., Magam, M.G., Qureshi, K.K.: Theoretical analysis of thulium doped fiber amplifier based on in-band pumping scheme. Microwave and Optical Technology Letters 63(4), 1309–1313 (2020). https://doi.org/10.1002/mop.32723

Optiwave: OptiSystem overview. https://optiwave.com/optisystem-overview/

Berkdemir, C., Ozsoy, S.: Modelling consideration of Praseodymium-doped fiber amplifiers for 1.3 μm wavelength applications. Optics Communications 269(1), 102–106 (2007). https://doi.org/10.1016/j.optcom.2006.07.054

Khamis, M.A., Sevilla, R., Ennser, K.: Large mode area Pr3+ doped chalcogenide PCF design for high efficiency mid-IR laser. IEEE Photonics Technology Letters 30(9), 825–828 (2018). https://doi.org/10.1109/LPT.2018.2818333

Kweon, G.I.: Noise figure of optical amplifiers. Journal of the Korean Physical Society 41(5), 617–628 (2002)

Khan, M.M., Sarma, K., Ali, K.: Optimization of O-band praseodymium- doped optical fiber amplifier in a CWDM communication link. In: 2024 ITU Kaleidoscope: Innovation and Digital Transformation for a Sustainable World (ITU K), pp. 1–5 (2024). https://doi.org/10.23919/ITUK62727.2024.10772774

Mohammed, D.Z., Hammadi, A.K.: Performance evaluation of O-band praseodymium-doped fiber amplifier with dual-pass regime. Fiber Integr. Opt. 41(5–6), 131–142 (2022). https://doi.org/10.1080/01468030.2022.2148143

Research funding: No funding was received for conducting this study.